

# Mean-field analysis of quantum phase transitions in a periodic optical superlattice

Arya Dhar<sup>1,\*</sup> and Manpreet Singh<sup>1,2,†</sup><sup>1</sup>Indian Institute of Astrophysics, II Block, Koramangala, Bangalore 560 034, India<sup>2</sup>School of Interdisciplinary and Transdisciplinary Studies, Indira Gandhi National Open University, New Delhi 110 068, IndiaRamesh V. Pai<sup>‡</sup>

Department of Physics, Goa University, Taleigao Plateau, Goa 403 206, India

B. P. Das<sup>§</sup>

Indian Institute of Astrophysics, II Block, Koramangala, Bangalore 560 034, India

(Received 15 June 2011; published 23 September 2011)

We analyze the various phases exhibited by a system of ultracold bosons in a periodic optical superlattice using the mean-field decoupling approximation. We investigate for a wide range of commensurate and incommensurate densities. We find the gapless superfluid phase, the gapped Mott insulator phase, and gapped insulator phases with distinct density wave orders.

DOI: [10.1103/PhysRevA.84.033631](https://doi.org/10.1103/PhysRevA.84.033631)

PACS number(s): 03.75.Nt, 05.10.Cc, 05.30.Jp

## I. INTRODUCTION

Mean-field theory has proven to be a useful tool for the analysis of the quantum phase transitions in lattice systems [1,2]. The zero-temperature phase diagram of the Bose-Hubbard model predicting the superfluid (SF) to Mott insulator (MI) transition was first discussed by Fisher *et al.* [3]. Jaksch *et al.* [2] suggested the possibility of such a transition in an optical lattice loaded with ultracold atoms and it was subsequently observed experimentally by Greiner *et al.* in 2002 [4]. There are a number of reviews on this topic [5–7]. Several versions of mean-field theory have been used in the context of ultracold atoms, including the Bogoliubov approximation [8], the Gutzwiller approach [2], and the mean-field decoupling approximation [9]. In the weak-interaction limit, the Bogoliubov approach is useful. However, it is not suitable for the study of the SF-MI phase transition since it is valid only for weak interactions. In the decoupling approximation, the Bose-Hubbard Hamiltonian is decoupled into single-site Hamiltonians. The resulting mean-field equation can be solved in two ways: either analytically using perturbation theory or numerically by diagonalizing the Hamiltonian matrix self-consistently using a convenient basis. The Gutzwiller mean-field approach has been used in several papers to study the Bose-Hubbard model in quantum lattices [2,10,11]. In this paper, we have applied the decoupling approximation to a  $d$ -dimensional periodic optical superlattice with a periodicity of two sites [12].

A number of papers on ultracold atoms in different types of optical superlattices have been published in the past few years [12–17]. Experiments on this subject have been proposed and carried out in different laboratories [18–20]. In this context, it is desirable to understand the possible phases in different kinds of optical superlattices. The main purpose of this study

is to understand the phases in the  $d$ -dimensional optical superlattice with a periodicity of two sites. For this purpose we use mean-field theory in the decoupling approximation to convert the full Hamiltonian into a sum of single-cell Hamiltonians. Our findings for ultracold atoms in the optical superlattice with a periodicity of two sites yields gapped insulators accompanied by different crystalline orders in addition to the usual Mott insulator and superfluid phases. These unusual insulating phases have been generically referred to as the superlattice-induced Mott insulators (SLMIs) in the literature [17]. Unlike the normal Mott insulator phase in which strong on-site interatomic interactions give rise to the gapped insulator, the SLMI phases arise due to the superlattice potential. Depending upon the distribution of bosons within the unit cell, there can be various types of SLMI phases. If the configuration of the occupancy of bosons within the unit cell is such that the alternate sites are occupied by one atom and the other being empty, then such an insulator is called SLMI-I. The configuration in which the alternate sites are occupied by two bosons and the other is empty is called SLMI-II. If the configuration is such that alternate sites are occupied by two bosons, and the other by one, then it is called SLMI-III.

The rest of the paper is organized in the following manner. In the next section, we describe the application of the mean-field decoupling approximation to an optical superlattice with a periodicity of two sites. In Sec. III we present our results. Our conclusions are given in Sec. IV.

## II. MEAN-FIELD CALCULATIONS FOR THE OPTICAL SUPERLATTICE

The system of bosons in a general optical superlattice can be best described by the Bose-Hubbard model as follows:

$$H = -t \sum_{\langle i,j \rangle} (\hat{a}_i^\dagger \hat{a}_j + \text{H.c.}) + \frac{U}{2} \sum_i \hat{n}_i (\hat{n}_i - 1) - \sum_i \mu_i \hat{n}_i. \quad (1)$$

In the above equation,  $\langle i, j \rangle$  denotes a pair of nearest neighbor sites  $i$  and  $j$ ,  $t$  denotes the hopping amplitude between adjacent

\*arya@iiap.res.in

†manpreet@iiap.res.in

‡rvpai@unigoa.ac.in

§das@iiap.res.in

sites,  $U$  represents the on-site interatomic interaction,  $\hat{a}_i^\dagger$  ( $\hat{a}_i$ ) is the creation (annihilation) operator which creates (destroys) an atom at site  $i$ ,  $\hat{n}_i = \hat{a}_i^\dagger \hat{a}_i$  is the number operator, and  $\mu_i$  represents the on-site chemical potential. For an optical lattice  $\mu_i = \mu$  for all  $i$ . However, this is not true for the optical superlattices and explicit dependence of  $\mu_i$  on the lattice site  $i$  depends on the specifics of the superlattices.

The most important step in obtaining the mean-field Hamiltonian is the decoupling of  $\hat{a}_i^\dagger \hat{a}_j$  into single-site operators. For this purpose, we make the following approximation:

$$a_i = \phi_i + \tilde{a}_i; a_i^\dagger = \phi_i^* + \tilde{a}_i^\dagger.$$

Here  $\phi_i = \langle a_i \rangle$  is the mean value and the superfluid order parameter, and  $\tilde{a}$  is the small fluctuation over the mean value. We assume  $\phi_i$  to be real [1]; hence,  $\phi_i = \phi_i^*$  for all  $i$ . Substituting the above approximation in the kinetic energy term of the Eq. (1), we get

$$\begin{aligned} -t \sum_{\langle i,j \rangle} (a_i^\dagger a_j + \text{H.c.}) &= -t \sum_{\langle i,j \rangle} (\tilde{a}_i^\dagger \tilde{a}_j + \tilde{a}_i \tilde{a}_j^\dagger) \\ -t \sum_{\langle i,j \rangle} (\tilde{a}_i^\dagger \phi_j + \tilde{a}_j \phi_i + \tilde{a}_i \phi_j + \tilde{a}_j^\dagger \phi_i + 2\phi_i \phi_j). \end{aligned} \quad (2)$$

We neglect the first term, which is second order in fluctuation. The validity of such an approximation can be assumed when  $t$  is small compared to the the interaction  $U$  and the superlattice potential  $\lambda$ . Defining  $\bar{\phi}_i = \frac{1}{z} \sum_\delta \phi_{i+\delta}$ ,  $\delta$  being summed over  $z = 2d$  nearest neighbors with  $d$  being the dimension of the optical lattice, we get the following mean-field Hamiltonian:

$$\begin{aligned} H^{MF} &= -tz \sum_i [\bar{\phi}_i (\tilde{a}_i^\dagger + \tilde{a}_i) + \bar{\phi}_i \phi_i] \\ &+ \frac{U}{2} \sum_i n_i (n_i - 1) - \sum_i \mu_i n_i. \end{aligned} \quad (3)$$

Substituting  $\tilde{a}_i = a_i - \phi_i$  in the above equation, we get

$$\begin{aligned} H^{MF} &= -tz \sum_i [\bar{\phi}_i (a_i^\dagger + a_i) - \bar{\phi}_i \phi_i] \\ &+ \frac{U}{2} \sum_i n_i (n_i - 1) - \sum_i \mu_i n_i, \end{aligned} \quad (4)$$

which can be written as a sum of single-site Hamiltonians, i.e.,  $H^{MF} = \sum_i H_i^{MF}$ , where

$$\frac{H_i^{MF}}{zt} = -\bar{\phi}_i (a_i^\dagger + a_i) + \bar{\phi}_i \phi_i + \frac{\tilde{U}}{2} n_i (n_i - 1) - \tilde{\mu}_i n_i. \quad (5)$$

We have divided the single-site mean-field Hamiltonian by  $zt$  to make it and other parameters dimensionless, and thus  $\tilde{U} = U/zt$  and  $\tilde{\mu}_i = \mu_i/zt$  are the dimensionless on-site interaction and chemical potential, respectively.

For an optical lattice, all the sites are equal, and thus  $\mu_i = \mu$  and  $\phi_i = \phi$  for all  $i$ . The Hamiltonian  $H_i^{MF}$  can then be diagonalized in the following manner. By assuming an initial value for the superfluid order parameter  $\phi$ , the matrix elements of the mean-field Hamiltonian are constructed in the number occupation basis  $|n\rangle$ , where  $n = 0, 1, 2, \dots, n_{\max}$ , where  $n_{\max}$  is the maximum number of bosons allowed per site whose value depends on the on-site interaction  $U$  and the chemical

potential  $\mu$ . Relatively small values of  $n_{\max}$  should suffice for large values of  $U$  and small values of  $\mu$  and vice versa. Since we have taken four different values of  $U$  ranging from 2 to 15 and the density is always less than 4, we have taken  $n_{\max} = 10$  in our calculation. The Hamiltonian matrix is then diagonalized to obtain the lowest eigenstate, which is used to obtain the new value for  $\phi$ . Using this value for  $\phi$ , the calculation is repeated till  $\phi$  is converged.

We now extend the mean field for the optical superlattice, which is formed by the superposition of two optical lattices with different wavelengths and a relative phase shift with respect to each other. This superlattice has a periodicity of two sites, and thus each unit cell consists of  $2^d$  sites with alternate sites having an energy shift  $\lambda_i$ . Such a system can be described by the Bose-Hubbard model (1) by taking into account the relative energy shifts of the potential minima such that  $\mu_i = \mu - \lambda_i$ , where  $\lambda_i$  denotes the energy shift and is called the superlattice potential.

In this optical superlattice, the sites are not equal since  $\mu_i = \mu - \lambda_i$  is not same for all  $i$ . However, the difference is restricted only within the unit cell and the whole system is built using this unit cell. The unit cell in the superlattice considered here consists of  $2^d$  sites. Since all dimensions are equivalent and the periodicity is two in our system, we can work on any one such direction, and hence we denote the two neighboring sites by 1 and 2. The mean-field Hamiltonian for such a unit cell can be written as

$$\begin{aligned} H_{uc}^{MF} &= -\bar{\phi}_2 (a_1^\dagger + a_1) - \bar{\phi}_1 (a_2^\dagger + a_2) + 2\bar{\phi}_1 \phi_2 \\ &+ \frac{\tilde{U}}{2} [n_1(n_1 - 1) + n_2(n_2 - 1)] \\ &- \tilde{\mu} [n_1 + n_2] + \tilde{\lambda}_1 n_1 + \tilde{\lambda}_2 n_2. \end{aligned} \quad (6)$$

In order to diagonalize the above Hamiltonian, we express all the operators including the Hamiltonian in the occupation number basis. Then we take initial guess values of the superfluid order parameters,  $\phi_1$  and  $\phi_2$ . After diagonalizing the  $H_{uc}^{MF}$  matrix using the standard Jacobi method, we find the ground-state energy and the ground-state wave function. From the relation  $\phi_i = \langle a_i \rangle$ , we calculate the superfluid order parameters using the ground-state wave function. We then substitute these new values of  $\phi_1$  and  $\phi_2$  in  $H_{uc}$  and iterate the process, until the values of  $\phi_1$  and  $\phi_2$  converge to  $10^{-6}$ . The different phases are then analyzed based on the values of these superfluid densities.

### III. RESULTS

Taking the superlattice potential for the two distinguished sites within the unit cell  $\lambda_1 = 0$  and  $\lambda_2 = \lambda$ , we present our results for a wide range of  $\lambda$ , densities  $\rho$ , and four characteristic values of the on-site interaction  $U$ , chosen to cover a substantial part of the phase diagram. In our analysis, we have taken  $zt = 1.0$ , so all quantities such as  $U$ ,  $\lambda$ , and  $\mu$  are expressed in units of  $zt$ .

First we investigate the effect of the superlattice potential on the superfluid phase. In Figs. 1 and 2, we plot, respectively, for  $U = 2$  the average density  $\rho$  and the superfluid density  $\rho^s$  as a function of the chemical potential  $\mu$  for different values of  $\lambda$  starting from 0.5 to 5.5 at an interval of 1.0. Here  $\rho$

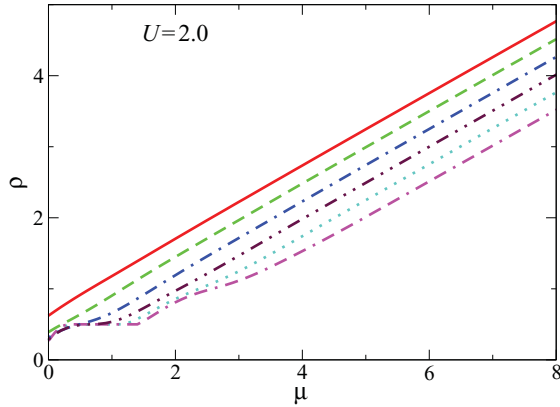


FIG. 1. (Color online) Variation of average density  $\rho$  as a function of the chemical potential  $\mu$  for  $U = 2$ , but for different values of  $\lambda$  starting from 0.5 (red solid curve) to 5.5 (magenta double dash dot curve) at the intervals of 1.0.

and  $\rho^s$  are, respectively, the average density and the superfluid density of a unit cell, i.e.,  $\rho = (\rho_1 + \rho_2)/2$ ,  $\rho^s = (\phi_1^2 + \phi_2^2)/2$ . It is known that for  $U = 2$ ,  $\lambda = 0$ , the model (1) is always in the superfluid phase [1] irrespective of the value of the density  $\rho$ .

From Figs. 1 and 2, we find that density  $\rho$  increases with an increase in  $\mu$  for finite, but small values of  $\lambda$ . The superfluid density  $\rho^s$  remains finite for all densities, which implies that the system continues to be in the superfluid phase as in the case of  $\lambda = 0$ . However, as  $\lambda$  is increased further, say, for example,  $\lambda = 4.5$ , the density develops a plateau at  $\rho = 1/2$  for a range of  $\mu$  values and vanishing compressibility  $\kappa = \frac{\partial \rho}{\partial \mu}$ . Figure 2 suggests vanishing superfluid density in the same range of  $\mu$ . For all other densities, i.e.,  $\rho \neq 1/2$ , including integer densities, the superfluid density remains finite. These features confirm that, for  $U = 2$ , model (1) is in the superfluid phase for all values of  $\rho \neq 1/2$  for all values of  $\lambda$ . However, for  $\rho = 1/2$  there is a superfluid to an insulator phase transition as  $\lambda$  is increased.

This insulator phase is different from the standard Mott insulator phase arising due to the on-site interaction. Here  $U = 2$  is small and the Mott insulator phase is not expected. The

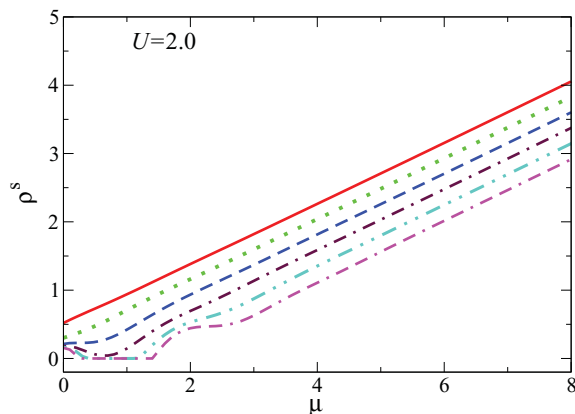


FIG. 2. (Color online) Variation of average superfluid density  $\rho^s$  as a function of  $\mu$  for the same set of parameters as in Fig. 1.

TABLE I. Results for  $U = 2.0$ .

$\lambda$	$\rho$	$\mu$	$\rho_1^s$	$\rho_2^s$	$n_1$	$n_2$
0.5	0.620	0.00	0.58	0.45	0.73	0.51
0.5	1.022	0.70	0.87	0.75	1.12	0.92
0.5	2.017	2.60	1.72	1.57	2.13	1.91
1.5	0.490	0.20	0.52	0.21	0.77	0.21
1.5	1.020	1.20	0.98	0.62	1.32	0.71
1.5	2.020	3.10	1.87	1.41	2.34	1.69
2.5	0.490	0.47	0.39	0.08	0.91	0.08
2.5	1.030	1.71	1.11	0.49	1.53	0.53
2.5	2.030	3.61	2.02	1.26	2.57	1.49
3.5	0.500	0.70	0.07	0.01	0.99	0.01
3.5	1.020	2.10	1.14	0.33	1.70	0.34
3.5	2.030	4.10	2.16	1.10	2.79	1.28
4.5	0.500	0.40	0.00	0.00	1.00	0.00
4.5	1.000	2.40	1.08	0.19	1.82	0.19
4.5	2.000	4.50	2.24	0.91	2.96	1.03
5.5	0.500	0.30	0.00	0.00	1.00	0.00
5.5	1.000	2.60	0.89	0.10	1.91	0.10
5.5	2.000	5.00	2.36	0.77	3.18	0.84

reason for the formation of an insulator phase for  $U = 2$  is due to the superlattice potential, and to distinguish this insulator from the Mott insulator phase, we call it a superlattice-induced Mott insulator [17] as mentioned earlier. In order to understand the SLMI phase, the distribution of bosons within the unit cell is tabulated in Table I. As we discussed in the previous section, the unit cell consists of  $2^d$  sites and each cell has two distinct sites, which we refer to as 1 and 2. The values of site densities  $\rho_1$  and  $\rho_2$  and superfluid densities  $\rho_1^s$  and  $\rho_2^s$  are listed in the table for different values of  $\lambda$ . For  $\lambda < 3.7$ , the on-site superfluid densities  $\rho_1^s$  and  $\rho_2^s$  remain finite for all densities. However, for  $\lambda \geq 3.7$  and density  $\rho = 1/2$ , we find  $\rho_1^s = \rho_2^s = 0$  and  $\rho_1 = 1, \rho_2 = 0$ . This implies, within the unit cell, that one site is occupied and the other is empty. Since this unit cell repeats to cover the entire lattice, it has every alternate site occupied with the other being empty like a charge density wave (CDW) phase, which normally arises due to nearest neighbor interaction. However, it should be noted

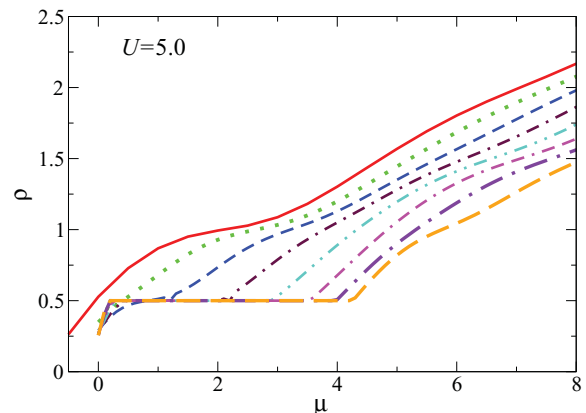


FIG. 3. (Color online) Variation of average density of a unit cell  $\rho$  as a function of the chemical potential  $\mu$  for  $U = 5$ , but for different values of  $\lambda$  starting from 0.2 (red solid curve) to 7.2 (orange large dashed curve) at intervals of 1.0.

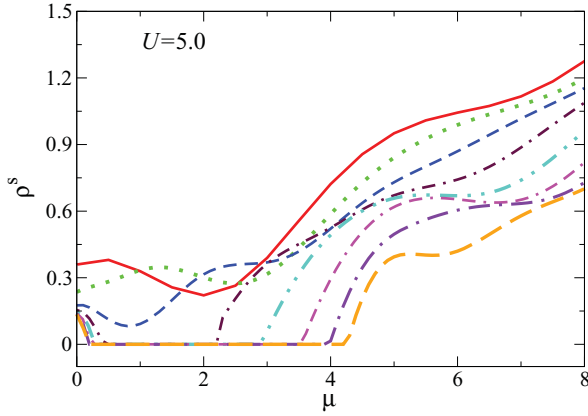


FIG. 4. (Color online) Variation of average superfluid density of a unit cell as a function of  $\mu$  for the same set of parameters as in Fig. 3.

here in this work that the CDW-like density distribution is due to the superlattice potential and there is no nearest neighbor interaction involved. Since the distribution of bosons follows a pattern  $[1\ 0\ 1\ 0\ 1\ 0\ \dots]$  in all  $d$  directions of the lattice, we call this phase SLMI-I to distinguish it from SLMI-II discussed below. Table I also confirms that there is no insulating phase for densities  $\rho = 1$  and 2.

Results for  $U = 5$  are similar to those of  $U = 2$ . In Figs. 3 and 4 we plot, respectively, density  $\rho$  and the superfluid density  $\rho^s$  as a function of  $\mu$  for different values of  $\lambda$ . The system is in the superfluid phase at  $\rho = 1/2$  and  $\rho = 1$  initially for low values of  $\lambda$  ( $< 2.6$ ). For  $\lambda > 2.6$ , a plateau appears in the  $\rho$  versus  $\mu$  plot for  $\rho = 1/2$ , suggesting a gap in the energy spectrum. The superfluid density vanishes in this region. This plateau at  $\rho = 1/2$  widens as  $\lambda$  increases. However, the system remains in the SF phase at  $\rho = 1$  for all the values of  $\lambda$  considered. In Table II, we tabulate the values of site densities and superfluid densities within the cell and we conclude that the transition from the SF to the SLMI-I phase is at  $\lambda = 2.6$ , when the superfluid density vanishes, and the occupancy configuration is of the form  $[1\ 0\ 1\ 0\ \dots]$ . On

TABLE II. Results for  $U = 5.0$ .

$\lambda$	$\rho$	$\mu$	$\rho_1^s$	$\rho_2^s$	$n_1$	$n_2$
0.2	0.523	0.0	0.370	0.35	0.57	0.48
0.2	1.030	2.5	0.270	0.26	1.03	1.02
0.2	2.080	7.5	1.190	1.17	2.09	2.06
2.2	0.500	0.9	0.110	0.06	0.95	0.06
2.2	1.010	3.3	0.433	0.36	1.13	0.90
2.2	2.000	8.1	1.250	1.09	2.19	1.81
3.2	0.500	0.5	0.000	0.00	1.00	0.00
3.2	1.000	3.8	0.570	0.42	1.22	0.78
3.2	2.010	8.7	1.350	1.08	2.30	1.73
4.2	0.500	0.2	0.000	0.00	1.00	0.00
4.2	0.990	5.3	0.790	0.29	1.65	0.34
4.2	2.010	10.2	1.540	0.91	2.62	1.40
7.2	0.500	0.2	0.000	0.00	1.00	0.00
7.2	1.010	5.8	0.620	0.18	1.82	0.20
7.2	2.020	10.7	1.54	0.83	2.73	1.30

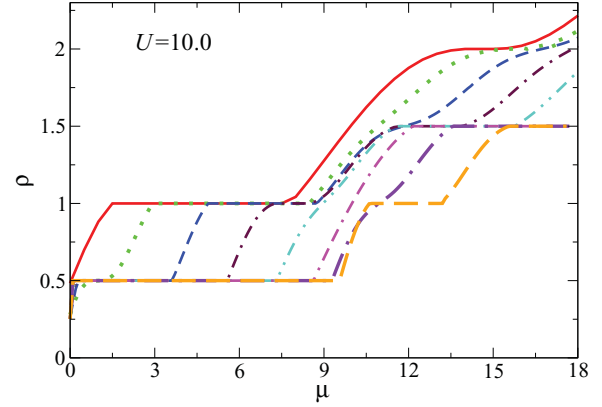


FIG. 5. (Color online) Variation of average density of a unit cell  $\rho$  as a function of the chemical potential  $\mu$  for  $U = 10$ , but for different values of  $\lambda$ , varying from 0.2 (red solid curve) to 14.2 (orange large dashed curve) at intervals of 2.0.

the other hand, at other values of  $\rho$  and for all values of  $\lambda$ , the superfluid densities  $\rho_1^s$  and  $\rho_2^s$  remain finite.

Results for  $U = 10$  are different from those of  $U = 5$ . This difference is mainly due to the fact that model (1) has SF to MI transitions for integer densities. For  $\rho = 1$ , the critical  $U_c \sim 5.8$  for the SF-MI transition [1] and this implies that, for  $U = 10$ , model (1) is in the Mott insulator phase for  $\rho = 1$ . In Figs. 5 and 6 we plot, respectively, density  $\rho$  and the superfluid density  $\rho^s$  as a function of  $\mu$  for different values of  $\lambda$ . From these figures the following conclusions are drawn. For small values of  $\lambda$ , the plateau in the  $\rho$  versus  $\mu$  plot exists only for  $\rho = 1$  and  $\rho^s$  vanishes in the same range of  $\mu$ , confirming the expected SF to MI transition for  $\rho = 1$ . The system remains in the superfluid phase for all other densities. However, as we increase  $\lambda$ , the plateau region at  $\rho = 1$ , i.e., the MI region, shrinks first, completely disappears for some values of  $\lambda$ , and reappears again for higher values of  $\lambda$ .

A plateau develops at  $\rho = 1/2$  for  $\lambda > 2.3$  and at  $\rho = 3/2$  for  $\lambda > 5.3$ . From the tabulated values of  $\rho_1$  and  $\rho_2$  in Table III, we see that the insulator phase at  $\rho = 1/2$  is the same as SLMI-I. The insulator phase at  $\rho = 3/2$  has a density distribution  $[2\ 1\ 2\ 1\ \dots]$ , which we call SLMI-III. The insulator phase at  $\rho = 1$  for higher values of  $\lambda$  has an occupation at alternate

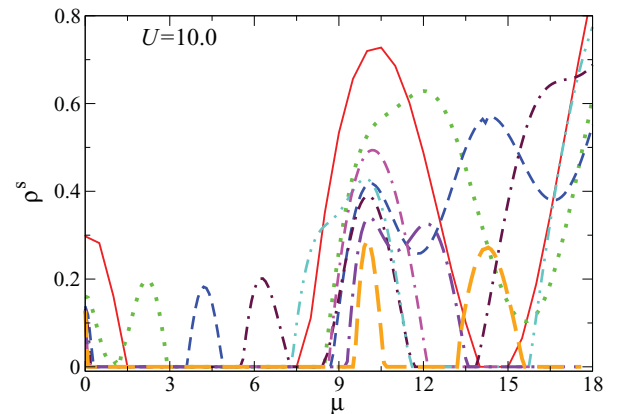


FIG. 6. (Color online) Variation of average superfluid density of a unit cell as a function of  $\mu$  for the same set of parameters as in Fig. 5.

TABLE III. Results for  $U = 10.0$ .

$\lambda$	$\rho$	$\mu$	$\rho_1^s$	$\rho_2^s$	$n_1$	$n_2$
0.2	0.48	0.00	0.30	0.29	0.53	0.44
0.2	1.00	2.00	0.00	0.00	1.00	1.00
0.2	2.00	14.50	0.00	0.00	2.00	2.00
2.2	0.50	1.20	0.00	0.00	1.00	0.00
2.2	1.00	3.00	0.00	0.00	1.00	1.00
2.2	2.00	15.00	0.00	0.00	2.00	2.00
6.2	0.50	0.50	0.00	0.00	1.00	0.00
6.2	1.00	7.50	0.00	0.00	1.00	1.00
6.2	1.50	12.00	0.00	0.00	2.00	1.00
10.2	0.50	0.19	0.00	0.00	1.00	0.00
10.2	1.00	9.97	0.65	0.32	1.51	0.47
10.2	1.50	12.16	0.00	0.00	2.00	1.00
14.2	0.50	0.10	0.00	0.00	1.00	0.00
14.2	1.00	10.70	0.00	0.00	2.00	0.00
14.2	1.50	15.60	0.00	0.00	2.00	1.00

lattice sites  $[2\ 0\ 2\ 0\ \dots]$ , which we refer to as the SLMI-II phase.

Thus, for  $U = 10.0$ , for  $\lambda < 2.3$  the system exhibits a Mott insulator phase for  $\rho = 1$  and a SF phase elsewhere. For  $2.3 < \lambda < 5.3$ , the system has two insulating phases: SLMI-I for  $\rho = 1/2$  and a MI phase for  $\rho = 1$ . The system is in the superfluid phase for the rest of the densities. For  $\lambda > 5.3$  the system shows SLMI-I for  $\rho = 1/2$ , a MI phase for  $\rho = 1$ , SLMI-III for  $\rho = 3/2$ , and SF for other densities. For  $\rho = 1$  the MI phase is lost for  $\lambda > 6.5$  and reappears as SLMI-II for  $\lambda > 13.1$ . The results for  $U = 10.0$  are in qualitative agreement with those obtained using Density Matrix Renormalization Group (DMRG) [17].

The system for  $U = 15.0$  behaves similarly to that for  $U = 10.0$ . At  $\rho = 1/2$ , the system starts off in the gapless SF phase for low values of  $\lambda$  ( $= 0.2$ ), as evident from Figs. 7 and 8 and Table IV. But at  $\rho = 1.0$  and  $2.0$ , the system is in the MI phase at this value of  $\lambda$ . As  $\lambda$  is increased to a value greater than  $2.2$ , a gap appears at  $\rho = 1/2$ , marking the transition from the SF to the SLMI-I phase, as seen in Table IV, where we have vanishing superfluid densities, and also a

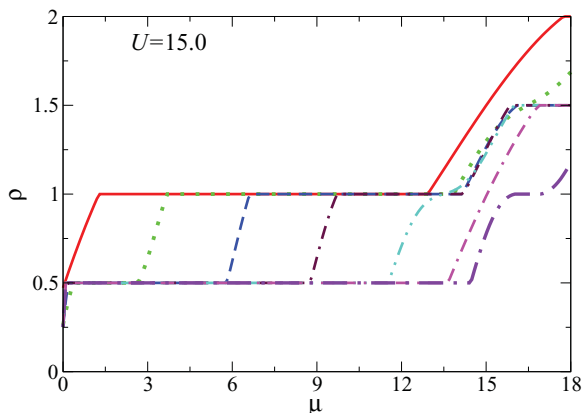


FIG. 7. (Color online) Variation of average density of a unit cell  $\rho$  as a function of the chemical potential  $\mu$  for  $U = 15$ , but for different values of  $\lambda$ , varying from 0.2 (red solid curve) to 18.2 (violet large dot dashed curve) at intervals of 3.0.

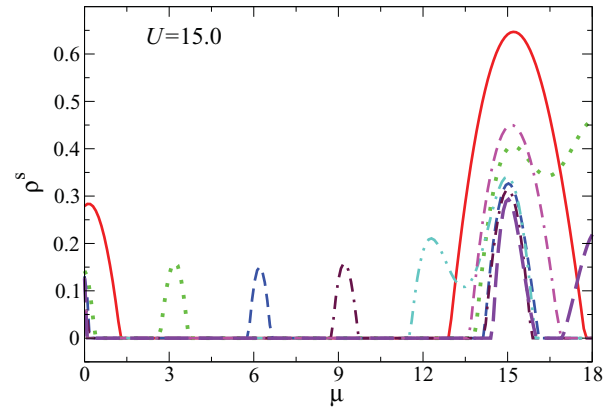


FIG. 8. (Color online) Variation of average superfluid density of a unit cell as a function of  $\mu$  for the same set of parameters as in Fig. 7.

occupancy configuration of  $[1\ 0\ 1\ 0\ \dots]$ . Also, at  $\rho = 3/2$ , another gap appears at  $\lambda = 4.8$ , implying the transition from the SF phase to the gapped SLMI-III phase with a configuration  $[2\ 1\ 2\ 1\ \dots]$ . As  $\lambda$  becomes greater than 11.7, the system at  $\rho = 1.0$  undergoes a phase transition from the MI to the SF phase, shown by the nonzero values of the superfluid density. As  $\lambda$  becomes beyond 18.1, the gap reappears once again, showing that the system has entered into the gapped SLMI-II phase with configuration  $[2\ 0\ 2\ 0\ \dots]$ .

#### IV. CONCLUSIONS

We have analyzed the various phases exhibited by a system of bosons in an optical superlattice with a unit cell consisting of two distinct lattice sites using the mean-field decoupling approximation, for various values of the superlattice potential,  $\lambda$ , corresponding to four values of the on-site interaction  $U$ . For  $U = 2.0$ , we find that the system resides in the SF phase for all densities for small values of  $\lambda$ . At  $\rho = 1/2$ , there is a transition from the SF to the SLMI-I phase at  $\lambda = 3.7$ , but for other densities, it remains in the gapless SF phase. For  $U = 5.0$ , the system undergoes a SF to SLMI-I phase transition for  $\rho = 1/2$  at  $\lambda = 2.6$ , but it remains in the SF phase for other densities and  $\lambda$ . For  $U = 10.0$ , the system undergoes a SF to SLMI-I phase transition at  $\lambda = 2.3$  for  $\rho = 1/2$ . However, for  $\rho = 1$ , the system starts in the MI

 TABLE IV. Results for  $U = 15.0$ .

$\lambda$	$\rho$	$\mu$	$\rho_1^s$	$\rho_2^s$	$n_1$	$n_2$
0.2	0.52	0.10	0.28	0.28	0.57	0.47
0.2	1.00	1.30	0.00	0.00	1.00	1.00
0.2	2.00	17.80	0.00	0.00	2.00	2.00
6.2	0.50	0.18	0.00	0.00	1.00	0.00
6.2	1.00	6.66	0.00	0.00	1.00	1.00
6.2	1.50	16.11	0.00	0.00	2.00	1.00
15.2	0.50	0.10	0.00	0.00	1.00	0.00
15.2	1.02	15.10	0.60	0.30	1.55	0.49
18.2	0.50	0.09	0.00	0.00	1.00	0.00
18.2	1.0	16.00	0.00	0.00	2.00	0.00
18.2	1.50	19.08	0.00	0.00	2.00	1.00

phase, as the value of  $U$  is large, and as  $\lambda$  is increased, the gap in the MI phase shrinks and eventually goes to zero, marking the MI-SF phase transition at  $\lambda = 6.5$ . The system stays in the gapless SF phase for  $6.5 < \lambda < 13.1$ . As  $\lambda$  is increased further the system undergoes a phase transition from SF to SLMI-II at  $\lambda = 13.1$ . For  $\rho = 3/2$ , we see a phase transition from SF to the SLMI-III phase at  $\lambda = 5.3$ . Similar behavior is observed for  $U = 15.0$ , with the system for  $\rho = 1/2$  undergoing a phase transition at  $\lambda = 2.2$ . For  $\rho = 1$ , the system makes a transition from the MI to the SLMI-I phase at  $\lambda = 11.7$ , and then from the SF to the SLMI-II phase at  $\lambda = 18.1$ . Also a phase transition is made from the SF to the SLMI-III phase at  $\lambda = 4.8$ . It should be possible to extend this calculation to superlattices with different periodicity. The charge density wave order in the SLMI phase will depend on the number of distinct sites within the unit cell. The mean-field approach

is exact for infinite dimensions, but the error, because of the neglect of the fluctuations, becomes severe in low dimensions [21]. However, it proves to be an excellent tool for qualitative analysis (e.g., analyzing the phase diagram), which is our focus in this paper. Since the parameters of the Hamiltonian can be varied over a large range of values by tuning the strength of the optical potentials, we hope our detailed study of model (1) will stimulate experimental studies that could lead to the observation of superlattice-induced Mott insulators.

#### ACKNOWLEDGMENTS

R.V.P. acknowledges financial support from CSIR and DST, India. We also acknowledge useful discussions with Tapan Mishra and Gora Shlyapnikov.

- 
- [1] K. Sheshadri, H. R. Krishnamurthy, R. Pandit, and T. V. Ramakrishnan, *Europhys. Lett.* **22**, 257 (1993).
  - [2] D. Jaksch, C. Bruder, J. I. Cirac, C. W. Gardiner, and P. Zoller, *Phys. Rev. Lett.* **81**, 3108 (1998).
  - [3] M. P. A. Fisher, P. B. Weichman, G. Grinstein, and D. S. Fisher, *Phys. Rev. B* **40**, 546 (1989).
  - [4] M. Greiner, O. Mandel, T. Esslinger, T. W. Hansch, and I. Bloch, *Nature (London)* **415**, 39 (2002).
  - [5] M. Lewenstein, A. Sanpera, V. Ahufinger, B. Damski, A. Sen De, and U. Sen, *Adv. Phys.* **56**, 243 (2007).
  - [6] I. Bloch, J. Dalibard, and W. Zwerger, *Rev. Mod. Phys.* **80**, 885 (2008).
  - [7] V. I. Yukalov, *Laser Phys.* **19**, 1 (2009).
  - [8] D. van Oosten, P. van der Straten, and H. T. C. Stoof, *Phys. Rev. A* **63**, 053601 (2001).
  - [9] R. V. Pai, K. Sheshadri, and R. Pandit, in *Current Topics in Atomic, Molecular and Optical Physics*, edited by C. Sinha and S. Bhattacharyya (World Scientific, Singapore, 2007), p. 105.
  - [10] W. Krauth, M. Caffarel, and J. P. Bouchaud, *Phys. Rev. B* **45**, 3137 (1992).
  - [11] D. S. Rokhsar and B. G. Kotliar, *Phys. Rev. B* **44**, 10328 (1991).
  - [12] B.-L. Chen, S.-P. Kou, Y. Zhang, and S. Chen, *Phys. Rev. A* **81**, 053608 (2010).
  - [13] V. G. Rousseau, D. P. Arovas, M. Rigol, F. Hebert, G. G. Batrouni, and R. T. Scalettar, *Phys. Rev. B* **73**, 174516 (2006).
  - [14] R. Roth and K. Burnett, *Phys. Rev. A* **68**, 023604 (2003).
  - [15] F. Schmitt, M. Hild, and R. Roth, e-print [arXiv:1005.3129v1](https://arxiv.org/abs/1005.3129v1) [cond-mat.quant-gas].
  - [16] G. Roux, T. Barthel, I. P. McCulloch, C. Kollath, U. Schollwöck, and T. Giamarchi, *Phys. Rev. A* **78**, 023628 (2008).
  - [17] A. Dhar, T. Mishra, R. V. Pai, and B. P. Das, *Phys. Rev. A* **83**, 053621 (2011).
  - [18] S. Piel, J. V. Porto, B. Laburthe Tolra, J. M. Obrecht, B. E. King, M. Subbotin, S. L. Rolston, and W. D. Phillips, *Phys. Rev. A* **67**, 051603(R) (2003).
  - [19] J. Sebby-Strabley, M. Anderlini, P. S. Jessen, and J. V. Porto, *Phys. Rev. A* **73**, 033605 (2006).
  - [20] P. Cheinet, S. Trotzky, M. Feld, U. Schnorrberger, M. Moreno-Cardoner, S. Fölling, and I. Bloch, *Phys. Rev. Lett.* **101**, 090404 (2008).
  - [21] R. V. Pai, K. Sheshadri, and R. Pandit, *Phys. Rev. B* **77**, 014503 (2008).